Comparison of broadband second-harmonic generation in periodically poled stoichiometric lithium tantalate with different magnesium oxide doping concentrations

XIAOLING ZHONG, MING YIN*, MENGXUE LIAN
School of Information Science and Technology, Chengdu University of Technology, Chengdu, 610059, China

Damage threshold of some periodically poled crystals can be improved by magnesium oxide doping , however, some properties of the crystals are also changed as a result of magnesium oxide doping. In this paper, type 0 quasi-phase matching (QPM) broadband second-harmonic generation (SHG) characteristics are compared in pure periodically poled stoichiometric lithium tantalate (PPSLT) and periodically poled 1 mol% magnesium oxide-doped stoichiometric lithium tantalate (1 mol% MgO:PPSLT). In both crystals, the group-velocity matching (GVM) fundamental wavelengths, QPM poling periods and SHG bandwidths are analyzed at room temperature, the tuning ranges of GVM fundamental wavelength are calculated with crystal temperature changing, the SHG bandwidths are obtained at different temperatures. The GVM fundamental wavelength in 1 mol% MgO:PPSLT appears little blue shift compared with that in PPSLT, the SHG bandwidth in 1 mol% MgO:PPSLT is a little narrower than that in PPSLT. There are some overlaps between tuning ranges of GVM fundamental wavelength in two crystals, the tuning range of GVM fundamental wavelength in 1 mol% MgO:PPSLT is wider than that in PPSLT. The results can be used to select different magnesium oxide-doped PPSLTs for different requirements QPM broadband SHG.

(Received April 07, 2016; accepted August 3, 2016)

Keywords: Broadband, Quasi-phase matching, Second-harmonic generation, Periodically poled lithium tantalate, Magnesium oxide doping

1. Introduction

The quasi-phase matching (QPM) second-harmonic generation (SHG) is widely used due to its simple structure and high efficiency. [1-5] In some applications like femtosecond laser and tunable laser SHGs and all optical wavelength conversion, the broadband SHG is needed. So QPM broadband SHG have attracted much attention in periodically poled lithium niobate (PPLN) [6-11], periodically poled lithium tantalate (PPLT) [12-14], periodically poled potassium niobate [15,16], periodically poled potassium titanyl phosphate [17-19] and orientation-patterned gallium arsenide [20].Damage threshold of some periodically poled crystals can be improve by magnesium oxide doping, however, some properties of the crystals are also changed as a result of magnesium oxide doping. The effect of magnesium oxide doping on QPM broadband SHG was investigated and it was found that the group-velocity matching (GVM) fundamental wavelength increases with the decrease of magnesium oxide doping in PPLN [9]. The crystal structure of PPLT is similar to that of PPLN, so the study on the effect of magnesium oxide doping on QPM broadband SHG in PPLT is significant.

In this paper, type 0 QPM broadband SHG characteristics are compared in pure periodically poled stoichiometric lithium tantalate (PPSLT) and periodically poled 1 mol% magnesium oxide-doped stoichiometric lithium tantalate (1 mol% MgO:PPSLT). In both crystals, the GVM fundamental wavelengths, QPM poling periods and SHG bandwidths are analyzed at room temperature (30 ℃), the tuning ranges of GVM fundamental wavelength are calculated with crystal temperature changing, the SHG bandwidths are obtained at different crystal temperatures. The GVM fundamental wavelength in 1 mol% MgO:PPSLT appears little blue shift compared with that in PPSLT, the SHG bandwidth in 1 mol% MgO:PPSLT is a little narrower than that in PPSLT, the tuning range of GVM fundamental wavelength in 1 mol% MgO:PPSLT is wider than that in PPSLT. The results can be used to select different magnesium oxide-doped PPSLTs for different requirements QPM broadband SHG.

2. Theoretical analysis

For collinear first-order QPM SHG, the wave vector mismatch Δk can be written as

$$\Delta k = k_s - 2k_f - \frac{2\pi}{\Lambda} \tag{1}$$

where k_s is the second-harmonic wave vector, k_f is the fundamental wave vector and Λ is the poling period.

There is a Λ which satisfies the QPM condition ($\Delta k = 0$) at every fundamental wavelength, the Λ is QPM Λ. The QPM Λ can be written as [8]

$$\Lambda = \frac{\lambda_f \lambda_s}{n_s \lambda_f - 2 n_f \lambda_s} \tag{2}$$

where λ_f is the fundamental wavelength, λ_s is the second-harmonic wavelength, n_f is the refractive index of fundamental wave and n_s is the refractive index of second-harmonic wave.

For QPM broadband SHG, Δk must satisfy $\Delta k = 0$ and $\frac{d\Delta k}{d\lambda_f} = 0$ simultaneously at some wavelength range. When $\frac{d\Delta k}{d\lambda_f} = 0$, λ_f satisfies the condition which is calculated as

$$\left(\frac{dn_s}{d\lambda_f} - \frac{dn_f}{d\lambda_f}\right)\lambda_f = (n_s - n_f) \tag{3}$$

from Equation (3), it can be derived that λ_f and λ_s satisfy GVM condition [8], the λ_f is GVM λ_f.

For type 0 QPM SHG, fundamental and second-harmonic waves are both extraordinary lights. n_f and n_s are given in [21,22].

3. Results and discussion

$\frac{d\Delta k}{d\lambda_f}$ and QPM Λ are calculated at different λ_f at room temperature in PPSLT, as shown in Fig. 1. (a) When $\frac{d\Delta k}{d\lambda_f} = 0$, λ_f and λ_s satisfy the GVM condition, the GVM λ_f is 2.564 μm, the QPM Λ at 2.564 μm is 34.70 μm. With a small signal approximation, the normalized SHG conversion efficiency η is proportional to $\mathrm{sinc}^2(\Delta kL/2)$, L is the crystal length. The SHG bandwidth is defined as the full width at half-maximum of the normalized SHG conversion efficiency η. [9] Fig. 1. (b) shows η as a function of λ_f with QPM Λ = 34.70 μm for a crystal length of 10 mm. The SHG bandwidth is 90 nm. The broadband SHG can be obtained at λ_f centered at 2.564 μm with SHG bandwidth 90 nm at room temperature in 10 mm long PPSLT.

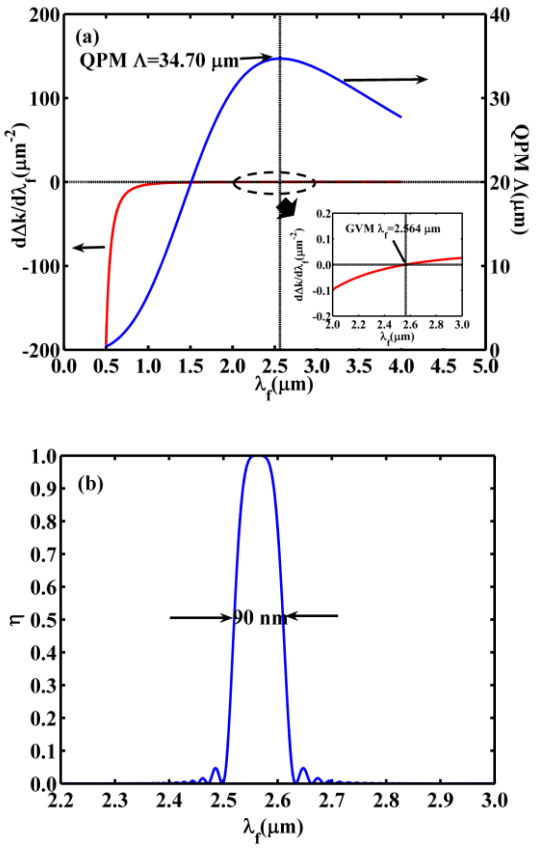

Fig. 1. (a) $\frac{d\Delta k}{d\lambda_f}$ and QPM Λ as a function of λ_f and (b) η as a function of λ_f with QPM Λ at the GVM λ_f at room temperature in PPSLT.

GVM λ_f and QPM Λ at the GVM λ_f are calculated from 30 ℃ to 170 ℃ in PPSLT, as shown in Fig. 2. The GVM λ_f increases from 2.564 to 2.590 μm and the QPM Λ at the GVM λ_f decreases from 34.70 to 34.33 μm with temperature increasing from 30 ℃ to 170 ℃. The tuning range of GVM λ_f is 26 nm.

Fig. 3 shows η as a function of λ_f with QPM Λ at the GVM λ_f at 80 ℃, 120 ℃ and 160 ℃ in 10 mm long PPSLT. GVM λ_f are 2.572, 2.580 and 2.588 μm at 80 ℃, 120 ℃ and 160 ℃, respectively. QPM Λ at 2.572, 2.580 and 2.588 μm are 34.58, 34.47 and 34.36 μm, respectively. The SHG bandwidth are 90 nm, 91 nm and 91 nm at 80 ℃, 120 ℃ and 160 ℃, respectively. From Fig.1. (b) and Fig.3, The SHG bandwidth increases very slightly with temperature increasing in PPSLT.

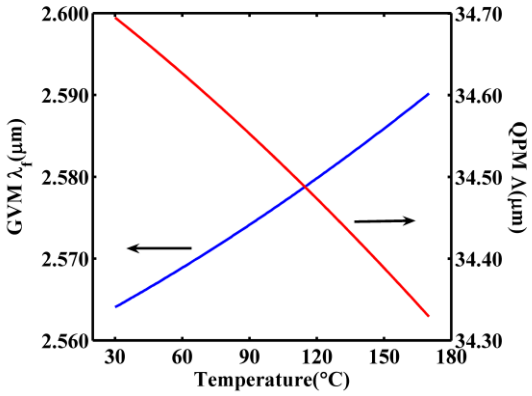

Fig. 2. GVM λ_f and QPM Λ at the GVM λ_f as a function of temperature in PPSLT.

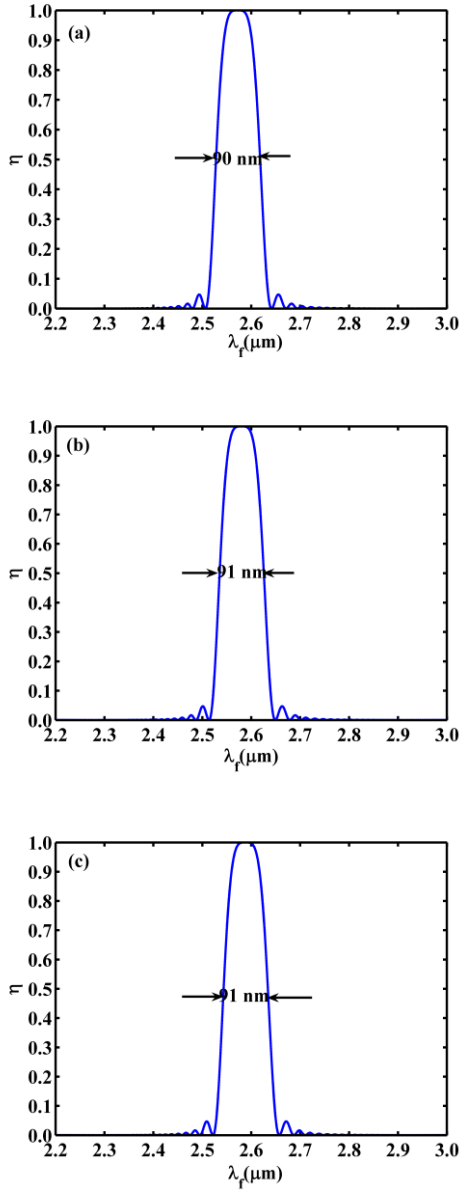

Fig. 3. η as a function of λ_f with QPM Λ at the GVM λ_f at (a)80 ℃, (b)120 ℃ and (c)160 ℃ in PPSLT.

$\frac{d\Delta k}{d\lambda_f}$ and QPM Λ are calculated at different λ_f at room temperature in 1 mol% MgO:PPSLT, as shown in Fig. 4. (a). The GVM λ_f is 2.545 μm, the QPM Λ at 2.545 μm is 34.98 μm. Fig. 4. (b) shows η as a function of λ_f with QPM Λ= 34.98 μm for a crystal length of 10 mm. The SHG bandwidth is 88 nm. The broadband SHG can be obtained at λ_f centered at 2.545 μm with SHG bandwidth 88 nm at room temperature in 10 mm long 1 mol% MgO:PPSLT.

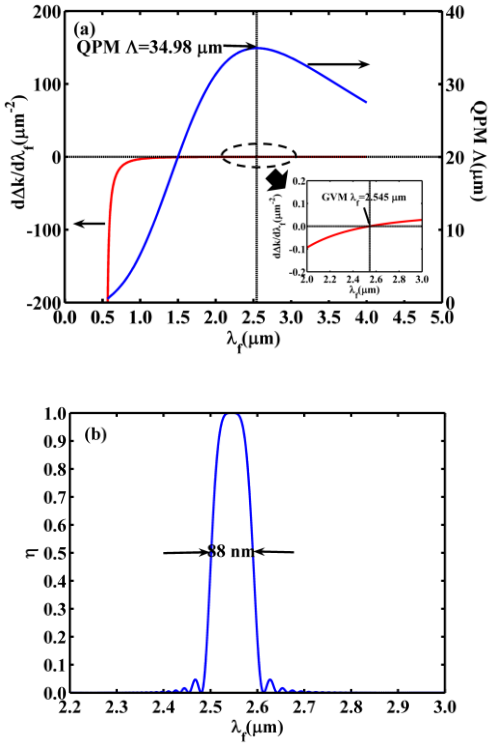

Fig. 4. (a) $\frac{d\Delta k}{d\lambda_f}$ and QPM Λ as a function of λ_f and (b) η as a function of λ_f with QPM Λ at the GVM λ_f at room temperature in 1 mol% MgO:PPSLT

GVM λ_f and QPM Λ at the GVM λ_f are calculated from 30 ℃ to 170 ℃ in 1 mol% MgO:PPSLT, as shown in Fig. 5. The GVM λ_f increases from 2.545 to 2.575 μm and the QPM Λ at the GVM λ_f decreases from 34.98 to 34.55 μm with temperature increasing from 30 ℃ to 170 ℃. The tuning range of GVM λ_f is 30 nm.

Fig. 6 shows η as a function of λ_f with QPM Λ at the GVM λ_f at 80 ℃, 120 ℃ and 160 ℃ in 10 mm long 1 mol% MgO:PPSLT. GVM λ_f are 2.555, 2.563 and 2.573 μm at 80 ℃, 120 ℃ and 160 ℃, respectively. QPM Λ are 34.84, 34.72 and 34.59 μm at 2.555, 2.563 and 2.573 μm, respectively. The SHG bandwidth are all 89 nm at 80 ℃, 120 ℃ and 160 ℃. From Fig. 4. (b) and Fig.6, the SHG bandwidth increases very slightly with temperature increasing in 1 mol% MgO:PPSLT.

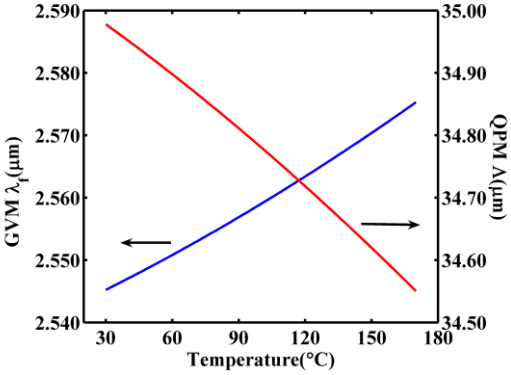

Fig. 5. GVM λ_f and QPM Λ at the GVM λ_f as a function of temperature in 1 mol% MgO:PPSLT

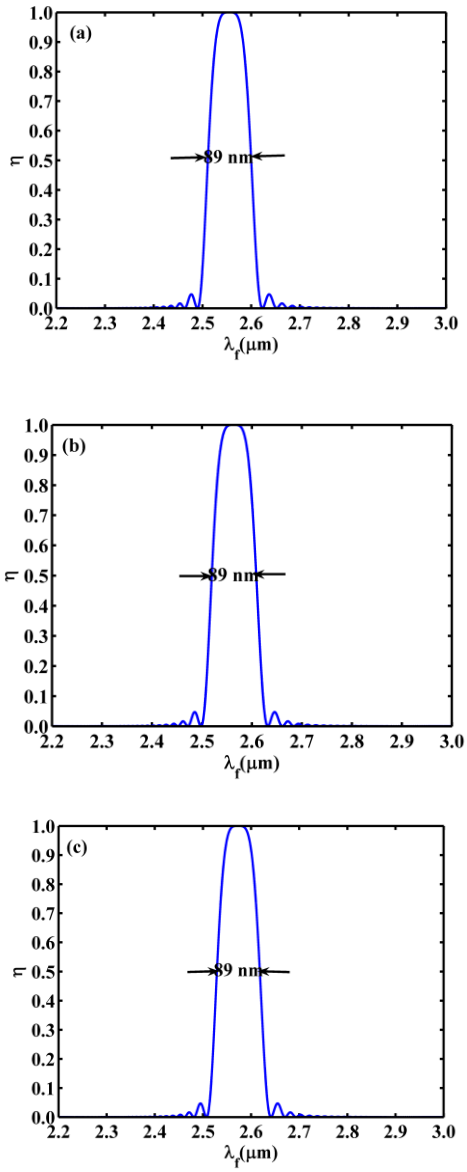

Fig. 6. H as a function of λ_f with QPM Λ at the GVM λ_f at (a)80 ℃, (b)120 ℃ and (c)160 ℃ in 1 mol% MgO:PPSLT

From Fig. 1 and Fig. 4, the GVM λ_f in 1 mol% MgO:PPSLT appears 19 nm blue shift compared with that in PPSLT at room temperature, the SHG bandwidth in 1 mol% MgO:PPSLT is 2 nm narrower than that in PPSLT for a crystal length of 10 mm at room temperature. From Fig. 2 and Fig. 5, there are some overlaps between tuning ranges of GVM λ_f in 1 mol% MgO:PPSLT and PPSLT, the tuning range of GVM λ_f in 1 mol% MgO:PPSLT appears little blue shift compared with that in PPSLT, the tuning range of GVM λ_f in 1 mol% MgO:PPSLT is 4 nm wider than that in PPSLT. From Fig.3 and Fig.6, the SHG bandwidth in 1 mol% MgO:PPSLT is 1, 2 and 2 nm narrower than that in PPSLT for a crystal length of 10 mm at 80 ℃, 120 ℃ and 160 ℃, respectively. The GVM λ_f in 1 mol% MgO:PPSLT appears little blue shift compared with that in PPSLT, the SHG bandwidth in 1 mol% MgO:PPSLT is a little narrower than that in PPSLT, the tuning range of GVM λ_f in 1 mol% MgO:PPSLT is wider than that in PPSLT. We try to explain such results. When magnesium oxide is doped in lithium tantalate, magnesium ions replace tantalate ions. Due to the difference between magnesium and tantalate ionic radii, the crystal structure is changed, the refractive index is altered slightly. The GVM fundamental wavelength and SHG bandwidth depend on refractive indices. Therefore, The GVM fundamental wavelength and SHG bandwidth are different in 1 mol% MgO:PPSLT and PPSLT.

4. Conclusion

In conclusion, we have studied type 0 QPM broadband SHG characteristics in PPSLT and 1 mol% MgO:PPSLT. The GVM fundamental wavelengths, QPM poling periods and SHG bandwidths are obtained at different temperature. The GVM fundamental wavelength in 1 mol% MgO:PPSLT appears little blue shift compared with that in PPSLT, the SHG bandwidth in 1 mol% MgO:PPSLT is a little narrower than that in PPSLT. There are some overlaps between tuning ranges of GVM fundamental wavelength in both crystals, the tuning range of GVM fundamental wavelength in 1 mol% MgO:PPSLT is wider than that in PPSLT. The results can be used to select different magnesium oxide-doped PPSLTs for different requirements QPM broadband SHG.

Acknowledgements

This work is supported by the National Natural Science Foundation of China (Grant No. 41304117), Cultivating Programme of Excellent Innovation Team of Chengdu University of Technology, and Provincial College Student Innovation and Entrepreneurship Training Program of Sichuan Province (Grant No. 201510616087).

References

[1] C. Lai, I. Hu, Y. Lai, Z. Huang, L. Peng, A. Boudrioua, A. Kung, Opt. Lett. **35**, 160 (2010).

[2] A. S. Aleksandrovsky, A. M. Vyunishev, A. I. Zaitsev, G. I. Pospelov, V. V. Slabko, Appl. Phys. Lett. **99**, 211105 (2011).

[3] L. Zhao, G. Yue, Y. Zhou, F. Wang, Opt. Express **21**, 17592 (2013).

[4] R. E. P. de Oliveira, C. J. S. de Matos, Opt. Express **21**, 32690 (2013) .

[5] A. Aadhi, N. A. Chaitanya, M. V. Jabir, R. P. Singh, G. K. Samanta, Opt. Lett. **40**, 33(2015).

[6] N. E. Yu, J. H. Ro, M. Cha, S. Kurimura, T. Taira, Opt. Lett. **27**, 1046 (2002).

[7] N. E. Yu, S. Kurimura, K. Kitamura, J. H. Ro, M. Cha, S. Ashihara, T. Shimura, K. Kuroda, T. Taira, Appl. Phys. Lett. **82**, 3388 (2003).

[8] M. Yin, S. Zhou, G. Feng, Acta Phys. Sin. **61**, 234206 (2012).

[9] J. Zhang, Y. Chen, F. Lu, W. Lu, W. Dang, X. Chen, Y. Xia, Appl. Optics **46**, 7791(2007).

[10] Z. Huang, C. Tu, S. Zhang, Y. Li, F. Lu, Y. Fan, E. Li, Opt. Lett. **35**, 877 (2010).

[11] S. Ashihara, T. Shimura, K. Kuroda, J. Opt. Soc. Am. B **20**, 853 (2003).

[12] M. Yin, J. Korean Phys. Soc. **67**, 1750 (2015).

[13] K. Lee, C. S. Yoon, F. Rotermund, Jpn. J. Appl. Phys. **44**, 1264 (2005).

[14] S. Stivala, A. C. Busacca, A. Pasquazi, R. L. Oliveri, R. Morandotti, G. Assanto, Opt. Lett. **35**, 363(2010).

[15] N. E. Yu, S. Kurimura, K. Kitamura, O. Jeon, M. Cha, S. Ashihara, T. Ohta, T. Shimura, K. Kuroda, J. Hirohashi, Appl. Phys. Lett. **85**, 5839 (2004).

[16] S. H. Bae, I. H. Beak, S. Y. Choi, W. B. Cho, F. Rotermund, C. S. Yonn, Opt. Commun. **283**, 1894 (2010).

[17] F. Konig, F. N. C. Wong, Appl. Phys. Lett. **84**, 1644 (2004).

[18] R. Wu, Y. Chen, J. Zhang, X. Chen, Y. Xia, Appl. Optics **44**, 5561(2005).

[19] F. Laurell, T. Calmano, S Muller, P. Zeil, C. Canalias, G. Huber, Opt. Express **20**, 22308 (2012).

[20] M. Yin, J. Optoelectron. Adv. Mat. **17**(9-10), 1253 (2015).

[21] A. Bruner, D. Eger, M. B. Oron, P. Blau, M. Katz, S. Ruschin, Opt. Lett. **28**, 194(2003).

[22] W. Weng, Y. Liu, X. Zhang, Chin. Phys. Lett. **25**, 4303(2008).

*Corresponding author: yinmingcdut@163.com